Development, Composition, and Structural Arrangements of the Ciliary Zonule of the Mouse

Yanrong Shi,[1] Yidong Tu,[2] Alicia De Maria,[1] Robert P. Mecham,[2] and Steven Bassnett[1,2]

[1]Department of Ophthalmology and Visual Sciences, Washington University School of Medicine, St. Louis, Missouri
[2]Department of Cell Biology and Physiology, Washington University School of Medicine, St. Louis, Missouri

Correspondence: Steven Bassnett, Department of Ophthalmology and Visual Sciences, Washington University School of Medicine, 660 S. Euclid Avenue, Campus Box 8096, St. Louis, MO 63110;
bassnett@vision.wustl.edu.

Submitted: January 7, 2013
Accepted: March 8, 2013

Citation: Shi Y, Tu Y, De Maria A, Mecham RP, Bassnett S. Development, composition, and structural arrangements of the ciliary zonule of the mouse. *Invest Ophthalmol Vis Sci*. 2013;54:2504–2515. DOI:10.1167/iovs.13-11619

Purpose. Here, we examined the development, composition, and structural organization of the ciliary zonule of the mouse. Fibrillin 1, a large glycoprotein enriched in force-bearing tissues, is a prominent constituent of the mouse zonule. In humans, mutations in the gene for fibrillin 1 (*FBN1*) underlie Marfan syndrome (MS), a disorder characterized by lens dislocation and other ocular symptoms.

Methods. Fibrillin expression was analyzed by in situ hybridization. The organization of the zonule was visualized using antibodies to Fbn1, Fbn2, and microfibril-associated glycoprotein-1 (Magp1) in conjunction with 5-ethynyl-2′-deoxyuridine (EdU), an S-phase marker.

Results. Microfibrils, enriched in Fbn2 and Magp1, were prominent components of the temporary vascular tunic of the embryonic lens. *Fbn2* expression by nonpigmented ciliary epithelial cells diminished postnatally and there was a concomitant increase in *Fbn1* expression, especially in cells located in valleys between the ciliary folds. Zonular fibers projected from the posterior pars plicata to the lens in anterior, equatorial, and posterior groupings. The attachment point of the posterior zonular fibers consisted of a dense meshwork of radially oriented microfibrils that we termed the fibrillar girdle. The fibrillar girdle was located directly above the transition zone, a region of the lens epithelium in which cells commit to terminal differentiation.

Conclusions. The development and arrangement of the murine ciliary zonule are similar to those of humans, and consequently the mouse eye may be a useful model in which to study ocular complications of MS.

Keywords: zonule, fibrillin, mouse

The zonule of Zinn is named for Johann Zinn, who described it in his 1755 monograph *Descriptio Anatomica Oculi Humani Iconibus Illustrata*.[1] The zonule, often referred to as the ciliary zonule, is the circumferential suspensory ligament that connects the lens of the eye to the ciliary body. The zonule is composed of an elaborate system of fibers that spans the gap between the lens and the adjacent nonpigmented ciliary epithelium (NPCE). This fibrous rigging ensures lens centration. In species that accommodate, the zonule transmits the forces that flatten the lens, allowing the eye to focus on distant objects.

For an anatomical feature first described more than 250 years ago, our understanding of the structure and composition of the ciliary zonule has emerged only slowly and to this day remains incomplete (see overviews of early research[2–4]). Histologically, the ciliary zonule belongs to a class of connective tissue elements called oxytalan fibers, a group that includes the periodontal ligament. Oxytalan fibers are characterized by their inability to take up aldehyde fuchsin stains unless first treated with strong oxidizing agents such as peracetic acid.[5] The difficulty in visualizing the zonule in histological sections is compounded by problems observing the zonule in the living eye, where the iris and sclera block direct observation. Dissection of the eye to expose the zonular fibers inevitably disturbs their three-dimensional organization. Similarly, analyses of fixed eyes by conventional[6–8] or environmental scanning electron microscopy,[9] while providing exquisitely detailed views, suffer from preparation artifacts associated with fixation and/or drying of the delicate fibrous material. Only with the introduction of noninvasive techniques, such as high-resolution ultrasound, has it been possible to visualize the organization of the zonule in undisturbed, living eyes.[10,11] Anatomical studies have focused on the organization of the ciliary zonule in humans and monkeys. The zonular apparatus in primates consists of a complicated arrangement of fibers that originate at the ciliary body and terminate on the lens capsule. Conventionally, the fibers are divided into anterior, equatorial, and posterior groupings, according to their point of attachment on the lens surface.[12] It is not known how this complicated rigging arises during development.

Fibrillin is a relatively recently identified component of the extracellular matrix.[13] It is a large (350-kDa) cysteine-rich glycoprotein and, along with microfibril-associated glycoprotein-1 (Magp1),[14] the principal structural component of the ciliary zonule.[15] Three fibrillin isoforms (fibrillin 1–3) are known in humans, although proteomic analysis of the zonule suggests that fibrillin-1 predominates.[15] Fibrillin is a common constituent of force-bearing structures such as blood vessels, lungs, and ligaments and is usually organized into 10- to 12-nm-diameter microfibrils.[16] Fibrillin can be found in association with an elastin core or, as in the ciliary zonule, in elastin-free bundles.[17] Mutations in the fibrillin-1 gene (*FBN1*) underlie

Copyright 2013 The Association for Research in Vision and Ophthalmology, Inc.

Marfan syndrome (MS), a disorder of connective tissue characterized by problems with skeletal, pulmonary, and cardiovascular systems. More than 600 different *FBN1* mutations have been identified to date.[18] People with MS are often unusually tall, with long limbs and long, thin fingers. Ocular manifestations of MS such as ectopia lentis and high myopia are common,[19] and both are included in the revised Ghent nosology for the disease.[20]

Unsurprisingly, biochemical and anatomical studies of the ciliary zonule have concentrated on the primate eye; relatively few studies have examined the ciliary zonule in the mouse. As a nocturnal animal with little or no accommodative ability, the mouse might seem an unpromising model for human ocular disease. However, mouse models of MS and other connective tissue disorders have begun to provide valuable insights into the role of fibrillin in human disease.[21] To fully utilize these powerful models in ocular studies requires a thorough analysis of fibrillin expression in the wild-type mouse eye and a careful assessment of the anatomy and composition of the ciliary zonule.

Materials and Methods

Animals

Wild-type mice (C57BL/6) or mT/mG fluorescent reporter mice ([B6.129(Cg)-*Gt(ROSA)26Sor*$^{tm4(ACTB-tdTomato,-EGFP)Luo}$/*J*]tdTomato) were obtained from the Jackson Laboratory (Bar Harbor, ME). The mT/mG mice express tandem dimer Tomato (tdTomato)[22] in cell membranes throughout the body.[23] Expression of tdTomato by ocular cells was used to visualize the complex structural arrangement of the folded ciliary epithelium and the organization of lens epithelial and fiber cells. Mice deficient in either Fbn2 or Magp1 were generated as previously described[24,25] and used to assess the specificity of antibody labeling in immunofluorescence experiments (see Supplementary Material and Supplementary Figs. S1, S2).

Animals were killed by CO_2 inhalation. Eyes were enucleated and processed for immunofluorescence or in situ hybridization experiments, as described below. All procedures described herein were approved by the Washington University Animal Studies Committee and were performed in accordance with the ARVO Statement for the Use of Animals in Ophthalmic and Vision Research.

Immunofluorescence

Enucleated eyes were fixed overnight in 4% paraformaldehyde/phosphate-buffered saline (PBS). The fixed tissue was rinsed in PBS and then dissected to remove the posterior globe to the level of the pars plana. Anteriorly, the cornea and iris were carefully removed. Dissected specimens thus consisted of rings of sclera with attached ciliary zonules and lenses. Nonspecific antibody binding was minimized by a 2-hour incubation in blocking solution containing 5% bovine serum albumin (BSA) in PBS. Samples were incubated overnight at 4°C in primary antibody diluted (1:50) in 2.5% BSA/PBS. After thorough washing in PBS, samples were incubated with appropriate fluorescently labeled secondary antibodies for 2 hours at room temperature. After final washing, samples were imaged by confocal microscopy, using a glass-bottomed viewing chamber, as described previously.[26] For each experiment, at least three animals (six eyes) were examined.

Antibodies

Anti-mouse fibrillin-2 (mFib2Gly) was generated against a truncated fibrillin-2–6His construct expressed in bacteria.[24] The construct contained exon 10 of mouse *Fbn2*, encoding the glycine-rich domain unique to this protein. Anti-mouse fibrillin-1 was generated as described[27] and generously provided by Dr. Lynn Sakai, Oregon Health Science University, Portland, Oregon. Goat polyclonal anti-MAGP1 was obtained from a commercial supplier (Cat. No. sc-50,084; Santa Cruz Biotechnology, Inc., Santa Cruz, CA). Alexa 488–conjugated chicken anti-goat and chicken anti-rabbit and Alexa 543– and Alexa 633–conjugated donkey anti-rabbit were obtained commercially (Invitrogen, Grand Island, NY) and used in appropriate combinations with the primary antibodies.

Cell Proliferation

S-phase cells were visualized following incorporation of 5-ethynyl-2′-deoxyuridine (EdU; Invitrogen, Carlsbad, CA), as previously described.[26] Cell nuclei were counterstained for 15 minutes in 1:1000 dilution (in PBS) of the far-red DNA dye DRAQ5 (Cell Signaling Technology, Inc., Danvers, MA).

Imaging

Confocal data sets were collected using a Zeiss 510 Meta confocal microscope (Carl Zeiss, Thornwood, NY) in the inverted configuration. Stacks of optical sections were visualized as maximum-intensity orthographic projections or rendered in three dimensions using the Simulated Fluorescence Process volume renderer (Scientific Volume Imaging, Hilversum, The Netherlands).

In Situ Hybridization

Mouse embryos or enucleated eye globes were fixed for 24 hours in 4% paraformaldehyde/PBS, embedded in paraffin, and sectioned in the midsagittal plane at 4 μm. In situ hybridization was carried out using the RNAscope technique (RNAscope 2.0; Advanced Cell Diagnostics, Hayward, CA), as described.[28] The mouse genome contains two fibrillin genes (*Fbn1* and *Fbn2*).[29] Target probe sets were generated against *Fbn1* and *Fbn2* transcripts. Each probe set consisted of 20 pairs of oligonucleotides spanning a ≈1-kb contiguous region of the target mRNA transcript (*Fbn1*, NM_007,993: 2290–3183; *Fbn2*, NM_010,181: 2933–3893). Following proprietary preamplification and amplification steps, target probes were detected using an alkaline-phosphatase–conjugated label probe with Fast Red as substrate and Gill's Hematoxylin as a counterstain. With this technique, individual mRNA molecules were detected as bright red puncta.[28] As a negative control, some sections were hybridized with target probe against *DapB*, a bacterial gene encoding dihydrodipicolinate reductase, a key enzyme in lysine synthesis. A target probe directed against ubiquitously expressed *PolR2A* (DNA-directed RNA polymerase II polypeptide A) served as a positive control. For each developmental stage, several sections from at least three animals were examined.

Results

Spatiotemporal Expression Pattern of Fibrillin Isoforms in the Developing Mouse Eye

At embryonic day 9.5 (E9.5), the earliest developmental stage examined, expression of *Fbn1* and *Fbn2* was almost undetectable in ocular structures (data not shown). However, by E12.5, both genes were expressed in the developing eye and elsewhere in the head (Fig. 1). *Fbn1* was expressed at relatively low levels in ocular tissue (Fig. 1A). In contrast, *Fbn2* expression was strong in the mesenchymal tissue surrounding the optic cup and in the

Investigative Ophthalmology & Visual Science

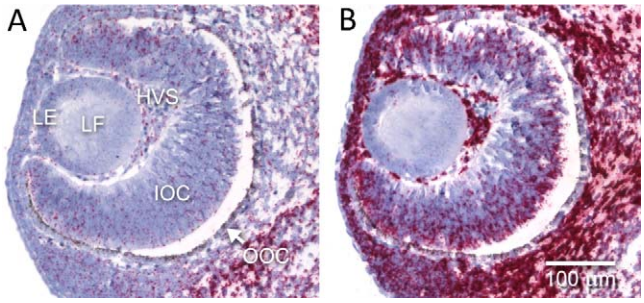

Figure 1. In situ hybridization analysis of *Fbn1* (**A**) and *Fbn2* (**B**) expression in the mouse eye at E12.5. Expression of *Fbn1* in the eye is low. *Fbn2*, however, is expressed moderately in the inner layer of the optic cup and strongly by cells of the developing hyaloid vascular system. LE, lens epithelium; LF, lens fibers; HVS, hyaloid vascular system; IOC, inner optic cup; OOC, outer optic cup. *Scale bar*: 100 μm.

hyaloid vascular system, which at this stage was developing around the lens (Fig. 1B). *Fbn2* expression level was moderate in the inner layer of the optic cup (which later forms the retina and NPCE) but weak in the outer layer (presumptive pigmented ciliary epithelium and retinal pigment epithelium). Neither the lens epithelium nor the primary lens fiber cells exhibited marked expression of *Fbn1* or *Fbn2*.

By E16.5, *Fbn1* was moderately expressed in the connective tissue coalescing around the eye (Fig. 2A). Within the eye, *Fbn1* expression was relatively low, with the strongest signal observed in the nonpigmented cells at the lip of the optic cup (Fig. 2C), the region in which the ciliary body and iris will later differentiate. Low-level expression was noted in the equatorial lens epithelium. For the most part, *Fbn2* was expressed in the same cells as *Fbn1*, but at significantly higher levels (Fig. 2B). *Fbn2* expression was most marked in the nonpigmented cells of the presumptive ciliary epithelium (Fig. 2D). *Fbn2* was also expressed strongly in cells located at the angle of the cornea and ciliary body, a region that, in adults, contains the ocular drainage structures. Compared to its expression levels in the anterior optic cup, *Fbn2* expression in the developing neural retina was low (Fig. 2D). At E12.5, cells of the hyaloid vascular system strongly expressed *Fbn2* (Fig. 1B); but, by E16.5, the vascular elements around the lens (posteriorly, the tunica vasculosa lentis and, anteriorly, the pupillary membrane) no longer expressed *Fbn1* or *Fbn2*.

At postnatal day 1 (P1), expression of *Fbn2* continued to dominate in the ciliary epithelium, but elsewhere in the eye, expression levels of *Fbn1* and *Fbn2* were comparable (Fig. 3). By this stage, the folds that characterize the adult ciliary epithelium had begun to form, and anteriorly, a subtle thinning of the nonpigmented epithelium represented the first morphological indication of iris differentiation.

In the eyes of 1-month-old (P30) mice, expression of fibrillin was markedly lower than at earlier developmental stages (Fig. 4). At this age, the NPCE was the only tissue to express fibrillin at high levels. In contrast to observations at earlier stages (Figs. 1–3), *Fbn1* expression at P30 exceeded that of *Fbn2* (compare

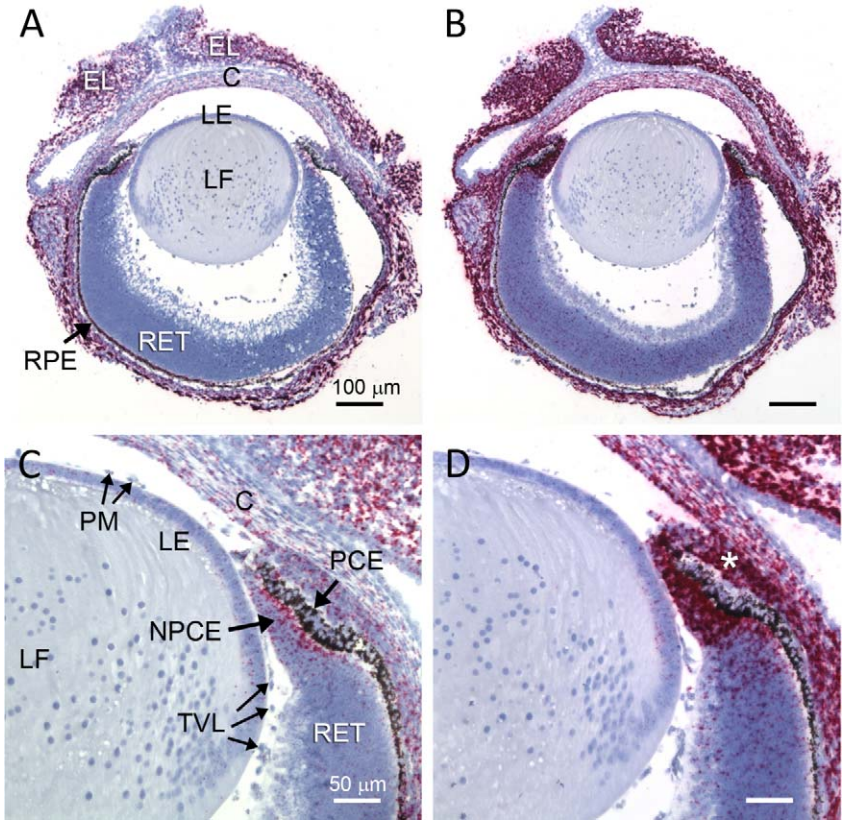

Figure 2. In situ hybridization analysis of *Fbn1* (**A**, **C**) and *Fbn2* (**B**, **D**) expression in the mouse eye at E16.5. *Fbn1* is expressed strongly in the connective tissue around the eye (**A**). Within the eye, modest expression is noted in the nonpigmented layer of the ciliary epithelium (**C**). *Fbn2* expression is strong in the cornea and connective tissues of the eye (**B**). Within the eye, *Fbn2* is expressed strongly by cells in the nonpigmented layer of the ciliary epithelium and in cells (*asterisk*) located in the angle between the ciliary body and cornea (**D**). EL, eyelid; C, cornea; LE, lens epithelium, LF, lens fiber cells; RET, retina; RPE, retinal pigmented epithelium; PCE, pigmented ciliary epithelium; NPCE, nonpigmented ciliary epithelium; TVL, tunica vasculosa lentis; PM, pupillary membrane. *Scale bar*: (**A**, **B**) = 100 μm; (**C**, **D**) = 50 μm.

Investigative Ophthalmology & Visual Science

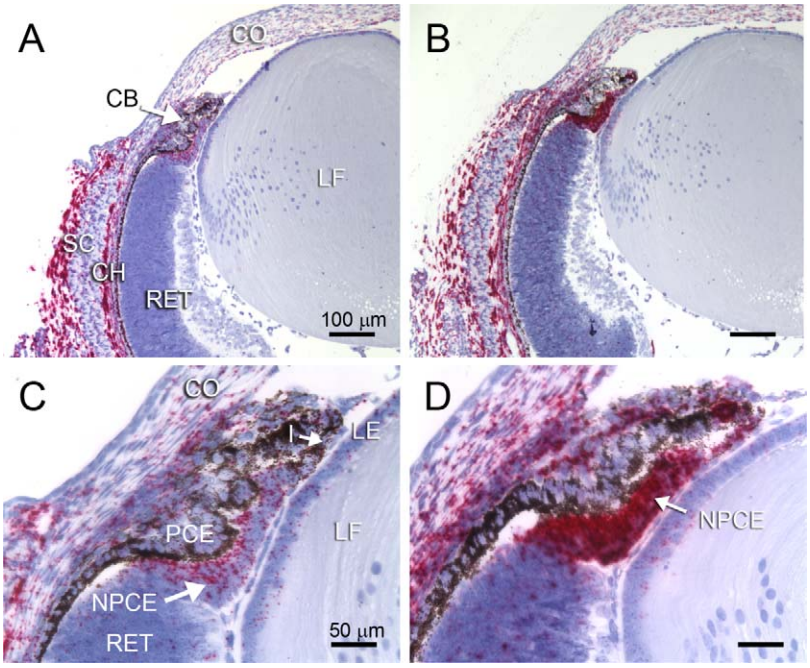

Figure 3. Expression of *Fbn1* (**A**, **C**) and *Fbn2* (**B**, **D**) in the 1-day-old (P1) mouse eye. *Fbn1* and *Fbn2* are expressed at comparable levels in cornea, choroid, and sclera (**A**, **B**). Although both genes are expressed in the nonpigmented layer of the developing ciliary epithelium (**C**, **D**), expression of *Fbn2* predominates (**D**). Expression levels of *Fbn1* and *Fbn2* in the neural retina are low compared to expression levels in the adjacent ciliary epithelium. CO, cornea; SC, sclera; CH, choroid; RET, retina; LE, lens epithelium; LF, lens fibers; PCE, pigmented ciliary epithelium; NPCE, nonpigmented ciliary epithelium; I, iris. *Scale bar*: (**A**, **B**) = 100 μm; (**C**, **D**) = 50 μm.

Figs. 4C, 4D). Furthermore, *Fbn1* expression was not uniform along the ciliary epithelium; it was markedly stronger in the region of the NPCE closest to the retina (Fig. 4C) and in cells located in the valleys between ciliary folds.

Microfibril Synthesis by Cells of the Developing Hyaloid Vasculature System

In mice and other mammals, the developing lens is temporarily nourished by an external vascular tunic that later regresses.[30] Posteriorly, the vascular system consists of the hyaloid artery and associated capillaries (vasa hyaloidia propria). Together, these extend from the optic disc to the lens, where they ramify to form a network of vessels (tunica vasculosa lentis; TVL) that covers the posterior lens surface. The anterior lens surface is supplied by an independent network of blood vessels, the pupillary membrane (PM). The capillaries of the PM are believed to be continuous with the iris vasculature.[30]

The capillaries of the PM and TVL are embedded in a loose extracellular matrix established at the surface of the lens capsule. Immunofluorescence analysis, using antibodies against the microfibril-associated glycoprotein Magp1, revealed that the matrix contained abundant microfibrils intimately associated with the capillaries (Fig. 5). Microfibrils were particularly numerous in regions of the matrix enriched in heparan sulfate proteoglycan 2 (perlecan; data not shown). Although not shown in Figure 5, the capillaries of the TVL were also embedded in a microfibril-rich matrix at the posterior lens surface.

In situ hybridization analysis suggested that fibrillin, the main structural component of microfibrils, was an abundant transcript in vascular cells surrounding the lens at E12.5 (Fig. 1B) and that, in those cells, *Fbn2* was the predominant isoform. Anti-fibrillin antibodies were used in conjunction with anti-Magp1 and endogenous TdTomato fluorescence to determine the relative abundance of Fbn1 and Fbn2 protein in microfibrils in the PM at P1 (Fig. 6). In accordance with the in situ hybridization analysis, the immunofluorescence experiments indicated that microfibrils associated with the PM and TVL were enriched in Fbn2, with relatively low levels of Fbn1 expression.

Development and Three-Dimensional Architecture of the Mouse Ciliary Zonule

Over the first few postnatal weeks, the capillaries of the PM and TVL regressed completely and, with them, the meshwork of Fbn2-rich microfibrils. As the microfibrils associated with the vasculature disappeared, a new set of fibrils emerged between the lens and the ciliary epithelium (Fig. 7). These represented the nascent ciliary zonule. At P1, Magp1-positive material was detected in the narrow cleft between the lens and the NPCE (Fig. 7B). At later stages (P30), sagittal sections through the eye revealed the deployment of the fan-shaped zonular apparatus (Fig. 7C). The adult zonular fibers have an elaborate three-dimensional organization best visualized in volumetric renderings generated from confocal image stacks (Fig. 7D). Such reconstructions suggested that the zonular fibers formed prominent anterior and posterior groupings that attached to the lens capsule on either side of the lens equator. Equatorial fibers were also present, but were fewer in number and less well organized than the anterior and posterior fibers. The zonular fibers appeared to attach directly to the surface of the lens capsule. Using XZ line scans collected perpendicular to the lens surface, we were unable to detect the penetration of fibers into the lens capsule (data not shown). Thus, in the mouse lens, unlike human lenses,[31] zonular fibers appear to adhere to, rather than penetrate, the capsule surface. A distinct difference was noted in the nature of the contact points for the anterior and posterior zonular fibers. The posterior fibers inserted into a dense meshwork of radially arranged microfibrils at the lens surface. This meshwork formed a ≈100-μm-

Investigative Ophthalmology & Visual Science

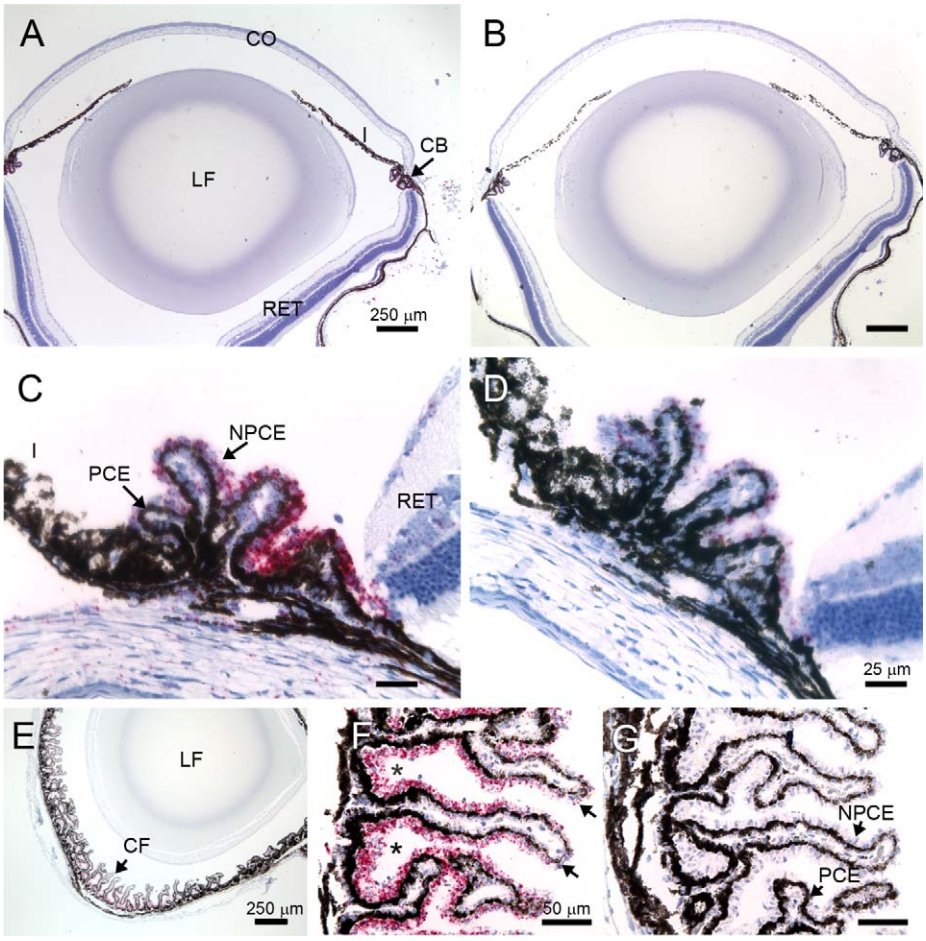

Figure 4. Expression of *Fbn1* (**A**, **C**, **E**, **F**) and *Fbn2* (**B**, **D**) in the 1-month-old (P30) mouse eye. Ocular expression of both genes is reduced relative to earlier developmental stages (**A**, **B**). Robust expression of *Fbn1* is observed in the posterior portion of the nonpigmented ciliary epithelium, near its border with the retina (**C**). In contrast, *Fbn2* expression in the ciliary epithelium is reduced to near-background levels (**D**). Sections through the ciliary body perpendicular to the optical axis reveal the elaborate folding pattern of the ciliary epithelium (**E**). *Fbn1* expression is not uniform in the NPCE, being stronger in the valleys (*asterisk*) than the peaks (*arrows*) of the folded epithelium (**F**). Hybridization with a probe set against *DapB*, a bacterial gene, serves as a negative control (**G**). CO, cornea; LF, lens fiber cells; CB, ciliary body; CF, ciliary folds; RET, retina; I, iris; PCE, pigmented ciliary epithelium; NPCE, nonpigmented ciliary epithelium. *Scale bar*: (**A**, **B**, **E**) = 250 μm; (**C**, **D**) = 25 μm; (**F**, **G**) = 50 μm.

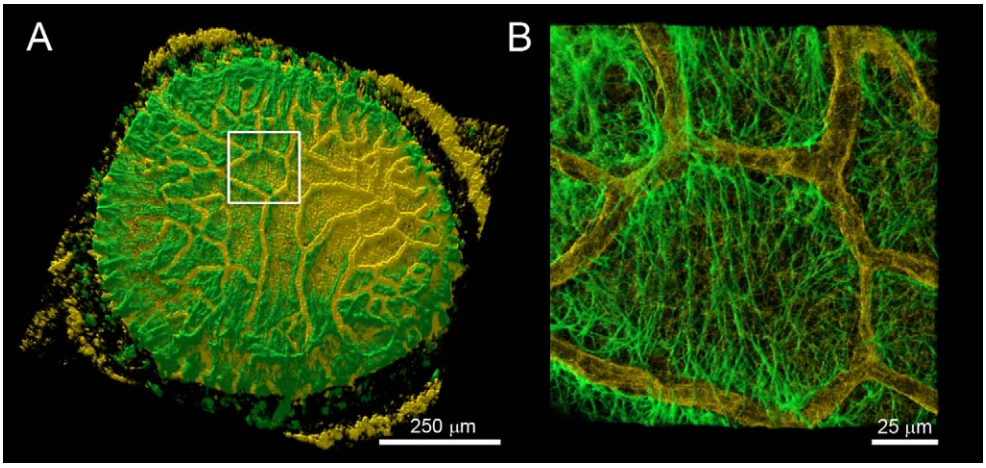

Figure 5. Microfibrils are abundant in the PM. En face view of the PM and underlying lens epithelium at the anterior surface of P1 mouse lens. (**A**) Low-magnification view. The arrangement of the capillaries is visualized using ubiquitously expressed, membrane-targeted tdTomato (*yellow*). Microfibrils (*green*) are visualized with anti-Magp1. The boxed region in (**A**) is shown at higher magnification in (**B**). Microfibrils span the gaps between the capillary elements and occasionally project over a capillary, but are not detected beneath capillaries. *Scale bar*: (**A**) = 250 μm; (**B**) = 25 μm.

Investigative Ophthalmology & Visual Science

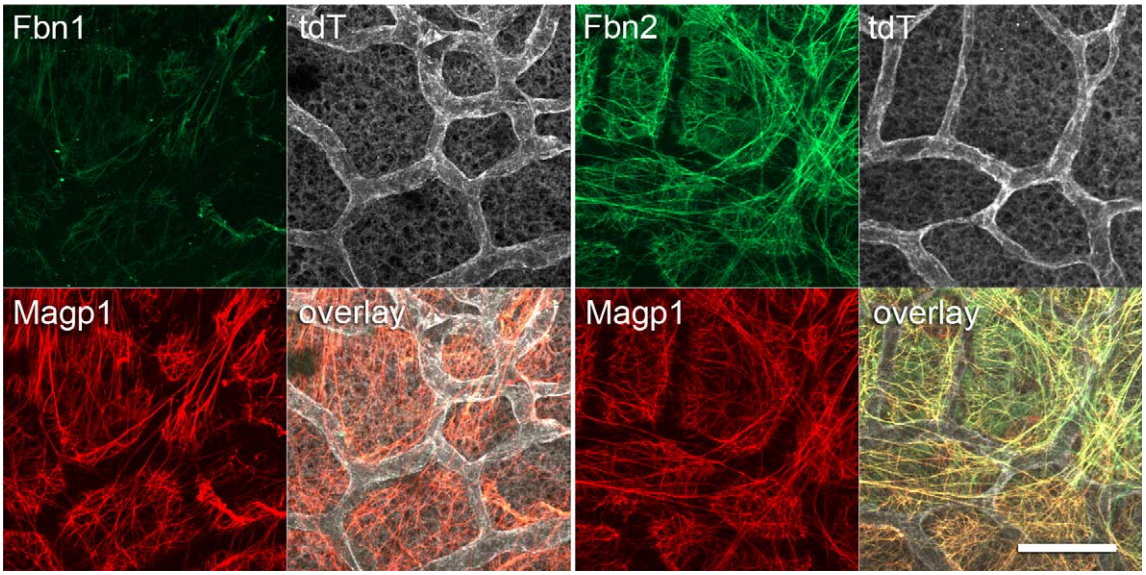

Figure 6. In the P1 mouse eye microfibrils in the PM are predominantly composed of Fbn2. The PM at the anterior surface of the mouse lenses was visualized using endogenously expressed tdTomato (*gray*), anti-Magp1 (*red*), and anti-fibrillin antibodies (*green*). PM microfibrils were identified using Magp1 immunofluorescence. Overlay of Magp1 immunofluorescence with either anti-Fbn1 or anti-Fbn2 revealed that Fbn2 was markedly more abundant in PM microfibrils than Fbn1. All images were collected using the same gain settings on the microscope. *Scale bar*: 50 μm.

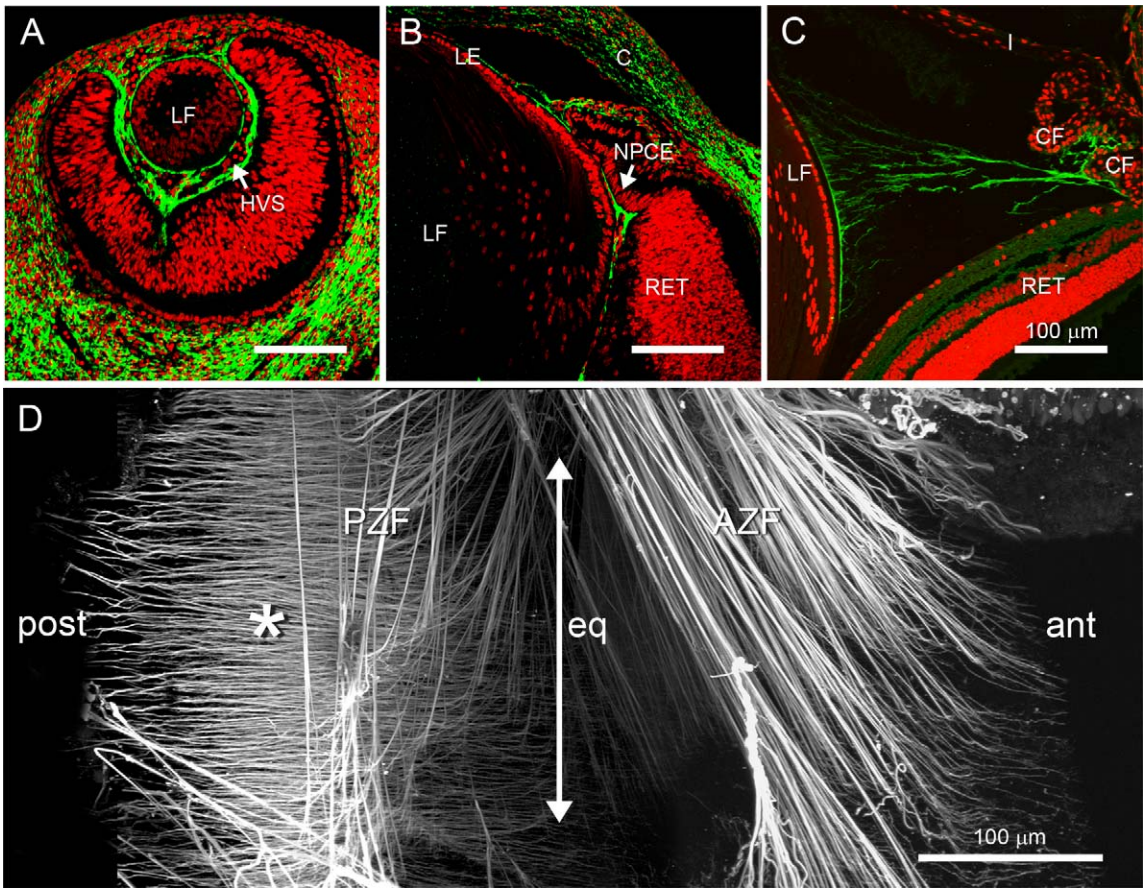

Figure 7. Emergence of the ciliary zonule during mouse development. Microfibrils (visualized using anti-Magp1 immunofluorescence [*green*] in paraffin-sectioned material) are present around the lens at E12.5, associated with the developing hyaloid vascular system (**A**). At P1, microfibril immunofluorescence (*green*) is detected in the narrow cleft between the lens and adjacent nonpigmented ciliary epithelium (**B**). By P30, the characteristic fan-shaped arrangement of zonular fibers is evident, extending from the folded ciliary epithelium to the lens equator (**C**). In the young adult lens (P60), the arrangement of the zonular fibers (visualized with anti-Magp1) is best appreciated in three-dimensional renderings of the equatorial lens surface (**D**). The fibers are arranged in two prominent groups: anterior zonule fibers and posterior zonule fibers. The anterior fibers terminate a short distance after their initial contact with the lens surface. In contrast, the posterior zonules form a dense fibrillar mesh (*asterisk*)

Investigative Ophthalmology & Visual Science

that girdles the lens immediately below the equator. LF, lens fibers; HVS, hyaloid vascular system; LE, lens epithelium; C, cornea; NPCE, nonpigmented ciliary epithelium; RET, retina; CF, ciliary folds; ant, anterior; post, posterior; AZF, anterior zonular fibers; PZF, posterior zonular fibers; eq, position and orientation of the lens equator. *Red* (**A–C**): nuclear fluorescence (DRAQ5); *green* (**A–C**): Magp1. *Scale bar*: (**A–D**) = 100 μm.

wide band that encircled the lens just below the equator. We refer to this structure as the fibrillar girdle. From the fibrillar girdle, individual fibrils sometimes extended several hundred micrometers across the surface of the posterior lens capsule. In contrast, the anterior zonule fibers ran only a short distance across the anterior capsule from the initial contact point.

Origin of Zonular Fibers on the Ciliary Body

The in situ hybridization data (Figs. 1–4) indicated that *Fbn1* and *Fbn2* transcripts were expressed specifically by cells of the NPCE, suggesting that those cells were the site of synthesis of zonular fibers. The three-dimensional structure of the ciliary epithelium is usually obscured by the lens and the zonular fibers. We therefore examined the ciliary epithelium in unfixed eyes, using endogenously expressed tdTomato to visualize the details of its undulating surface (Fig. 8A). Three-dimensional reconstructions revealed that the epithelium was arranged in a series of irregular radial folds, with a peak-to-peak periodicity of 50 to 100 μm. Unlike the human ciliary epithelium, the mouse epithelium was not subdivided into anatomically distinct pars plicata and pars plana regions. In the mouse, the pars plana was vestigial or absent and the folds of the pars plicata merged directly with the adjacent retina. We next examined the ciliary body from its anterior aspect in fixed preparations from which the cornea and iris had been removed (Fig. 8B). The anterior zonular fibers were clearly visible in this orientation. Although a few fibers originated from the anterior surface of the ciliary epithelium, it was evident that the great majority projected from the posterior aspect of the ciliary epithelium. Consequently, the zonular apparatus was imaged from the posterior aspect (Figs. 8C, 8D). Three-dimensional renderings of the posterior zonular apparatus revealed that most fibers originated at the distal region of the pars plicata, close to its junction with the retina (Fig. 8C). The ciliary folds in this region were covered with a dense meshwork of fibrils from which zonular fibers projected to the lens (Fig. 8D). In high-magnification views, the spatial relationship between the fibrillar girdle and the underlying lens cells could be discerned. The fibrillar girdle was located at the interface between the irregularly packed epithelial nuclei and the radially arranged fiber cell nuclei.

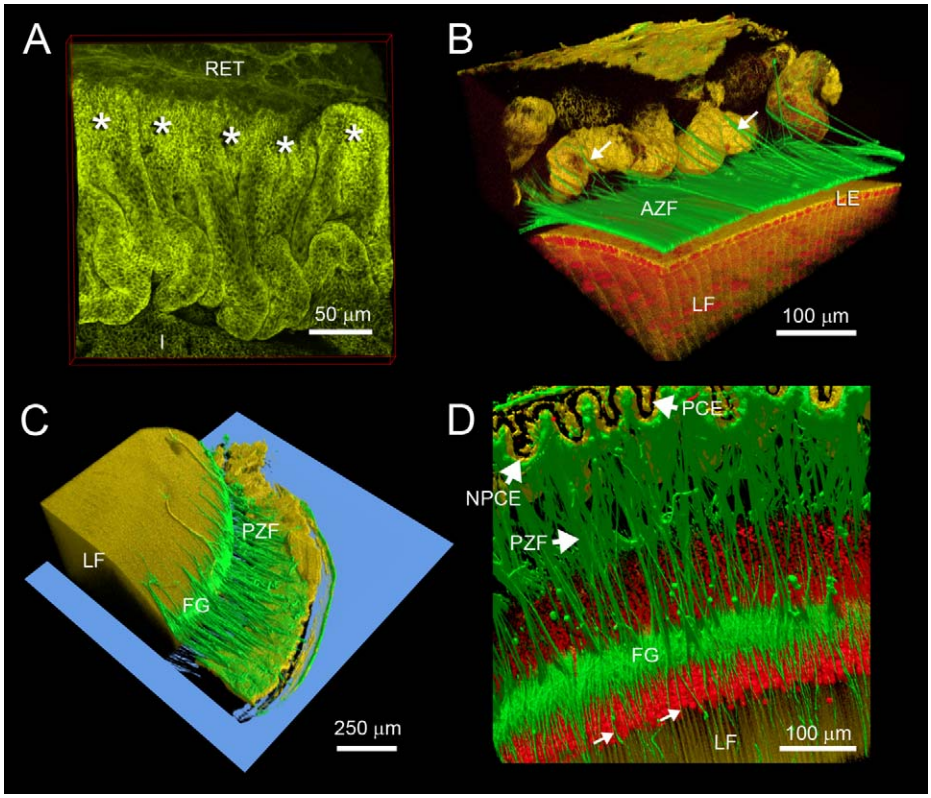

Figure 8. Origin and termination points of zonular fibers in the mouse eye. En face views show that the ciliary epithelium is folded into irregular pleats (**A**). The folded region of the ciliary epithelium (pars plicata) fuses directly with the retina. Zonular fibers are not visible in this unstained, unfixed preparation. Most zonular fibers originate from the zone marked with *asterisk*. Although a few anterior zonular fibers can be traced to origin points on the anterior surface of the ciliary epithelium (*arrows*), most extend from the posterior portion of the NPCE (**B**). Zonular fibers do not project from the innermost tips of the ciliary epithelium but rather originate in the posterior pars plicata region (**C**). Higher-magnification views (**D**) show posterior zonular fibers extending from the posterior pars plicata to termination points on the lens fibrillar girdle. Some fibrils (*small arrows*) extend posteriorly from the fibrillar girdle and run for several hundred micrometers across the posterior surface of the lens capsule. RET, retina; I, iris; AZF, anterior zonular fibers; PZF, posterior zonular fibers; LE, lens epithelium; LF, lens fiber cells; FG, fibrillar girdle; PCE, pigmented ciliary epithelium; NPCE, nonpigmented ciliary epithelium. (**A**) is from a P14 mouse; (**B–D**) are from P30 mice. *Scale bar*: (**A**) = 50 μm; (**B**, **D**) = 100 μm; (**C**) = 250 μm.

Investigative Ophthalmology & Visual Science

The in situ hybridization data indicated a developmental switch in fibrillin isoform expression in the NPCE. Early in development, *Fbn2* was the more abundant transcript (Figs. 2, 3), whereas, at later stages, *Fbn1* was the predominant isoform (Fig. 4). Assuming that zonular fibers grow by addition of subunits to their proximal ends, isoform switching is expected to result in fibers that are enriched in Fbn1 near the ciliary epithelium and in Fbn2 near the lens. We used a double-labeling strategy (with anti-Fbn1 or anti-Magp1) to test whether this was the case (Fig. 9). As expected, Magp1 labeled the entire length of zonular fibers in P30 mouse eyes. Fbn1 expression followed a similar pattern, although the staining intensity was somewhat reduced in the zonular fibers on the posterior lens capsule. Surprisingly, Fbn2 immunofluorescence was restricted to the proximal region of the zonular fibers, near their origin point on the ciliary epithelium.

Relationship Between the Fibrillar Girdle and the Proliferation/Differentiation Compartments of the Lens Epithelium

The lens is a polarized structure containing mitotically active epithelial cells at the anterior surface and terminally differentiated lens fiber cells at the posterior. Epithelial cell division is restricted to a band of cells near the equatorial margin of the epithelium called the "germinative zone" (GZ).[32] Once cells have passed through the germinative zone they enter the "transition zone" (TZ),[33] a region ≈10 cells wide, populated by cells that have withdrawn from the cell cycle and committed to terminal differentiation.[33] Finally, under the influence of factors present in the vitreous humor, most notably fibroblast growth factor,[34] lens cells terminally differentiate, a process that among other things involves enormous cellular elongation and the synthesis of high concentrations of crystallin proteins. The highest density of microfibrils on the lens surface was detected in the fibrillar girdle, the attachment point for the posterior zonular fibers. To localize the position of the fibrillar girdle with respect to the proliferation/differentiation compartments of the lens, we reconstructed the zonular apparatus in eyes in which S-phase cells had been prelabeled with EdU (Fig. 10). Almost all (>95%) S-phase lens cells were located in the region of the epithelium spanned by the anterior and posterior zonule fibers. The fibrillar girdle was located directly above the TZ. No S-phase cells were detected beneath the fibrillar girdle.

Discussion

Previous anatomical studies of the ciliary zonule have relied on conventional histological analysis of sectioned material or scanning electron microscopy of surface structures. Here, we utilized confocal microscopy to visualize the three-dimensional organization of the ciliary zonule in the mouse eye. This approach, in conjunction with a novel in situ hybridization technique and immunofluorescence analysis using antibodies raised to microfibril components, allowed us to gain insights into the development and organization of the mouse ciliary zonule.

The arrangement of murine zonular fibers appeared grossly similar to that in human and monkey eyes,[11,12] with well-defined anterior, equatorial, and posterior sets. In primate eyes, the zonular fibers play a key role in accommodation. They transmit the forces that flatten the lens, allowing the eye to focus on distant objects. The mouse eye is not thought capable

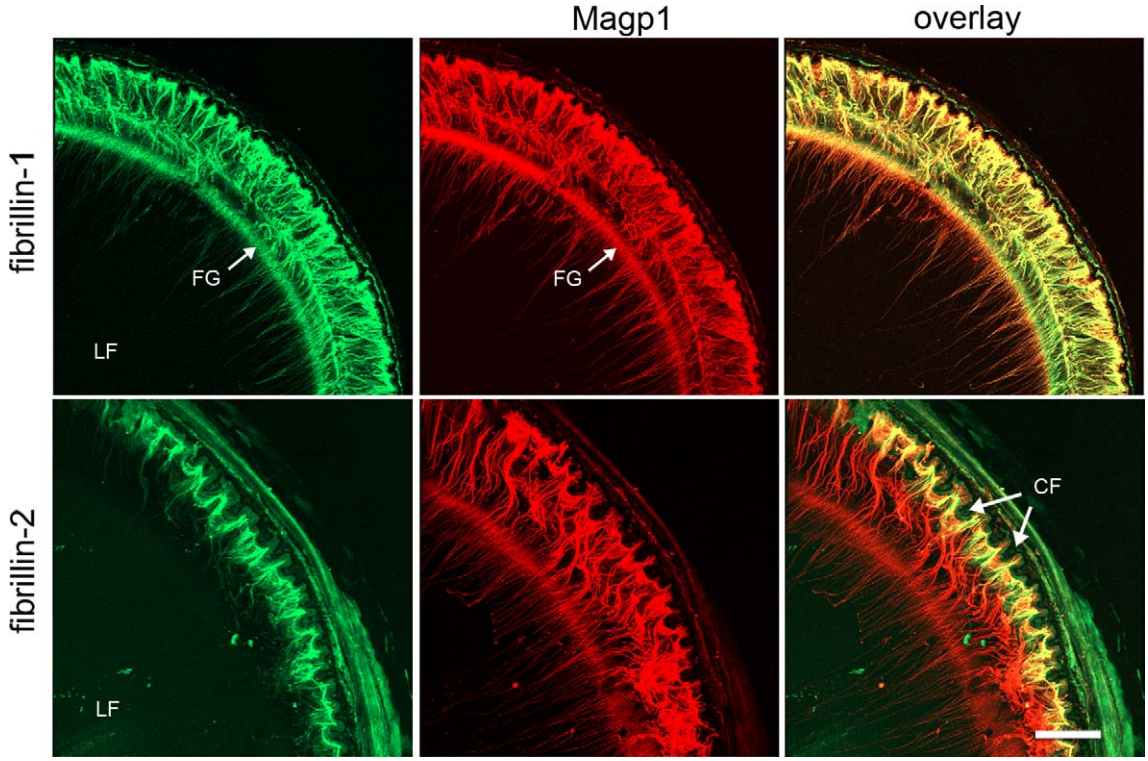

Figure 9. Fibrillin isoform expression along the posterior zonular fibers in 1-month-old mice. The ciliary body and attached lens are shown from the posterior aspect. Zonular fibers are visualized with anti-Magp1 in combination with either anti-Fbn1 or anti-Fbn2. Fbn1 is detected along the entire length of the zonular fibers, although there is a decrease in staining intensity relative to Magp1 in fibers projecting from the fibrillar girdle across the posterior lens capsule. In contrast, strong Fbn2 immunofluorescence is detected only in the vicinity of the ciliary folds. Neither the fibrillar girdle nor the fibers on the posterior capsule are stained by anti-Fbn2. LF, lens fibers; FG, fibrillar girdle; CF, ciliary folds. *Scale bar*: 100 μm.

Investigative Ophthalmology & Visual Science

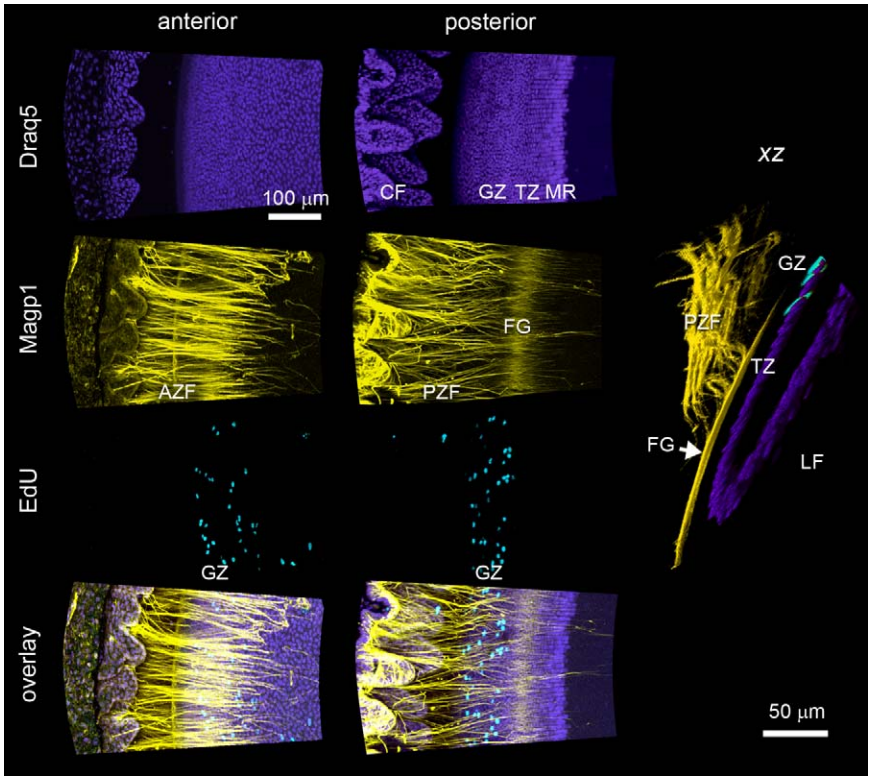

Figure 10. Spatial relationship between ciliary zonule and the proliferative/differentiation compartments of the lens. The zonular apparatus of a 1-month-old mouse is shown from anterior, posterior, and XZ aspects. Tissue was stained with DRAQ5 (*purple*) to visualize nuclei, anti-Magp1 (*yellow*) to visualize ciliary zonules, and EdU (*light blue*) to identify S-phase cells. Almost all (>95%) S-phase lens epithelial cells are located in the zone spanned by the attachments of the anterior and posterior zonule fibers. From the posterior aspect, the fibrillar girdle is evident as a band of dense, radially oriented fibrils encircling the lens. En face or XZ projections of this region reveal that the fibrillar girdle attaches to the lens surface directly above the lens transition zone, the region in which cells withdraw from the cell cycle and commit to differentiate. CF, ciliary folds; GZ, germinative zone; TZ, transition zone; MR, meridianal rows; FG, fibrillar girdle; PZF, posterior zonular fibers; AZF, anterior zonular fibers; LF, lens fibers.

of accommodation, implying that the complex rigging of zonular fibers functions primarily in lens centration and that a role in accommodation may have emerged later in evolution.

In principle, zonule components could be derived from cells in lens, the ciliary body, or both. Relatively few studies have examined fibrillin gene expression in the eye. However, studies in guinea pig[35] and, more recently, in humans[31] have suggested that *Fbn1* expression is restricted to cells of the NPCE, a finding supported by the current study. An age-dependent decline in fibrillin mRNA levels was also a consistent finding in the three investigations (although our study suggested that *Fbn1* transcripts were still present in the NPCE of 1-month-old animals) and may suggest that the rate of synthesis of zonule proteins slows with age. Consistent with this notion, incorporation of radiolabeled amino acid precursors into the ciliary zonule was undetectable beyond 30 days in mice.[36] Proteomic analysis has indicated that Magp1 is the principal microfibril-associated component in zonular fibers,[15] consistent with the results of our immunofluorescence studies. Unlike Fbn1 and Fbn2, which appear to be produced exclusively by the ciliary epithelium, Magp1 may be synthesized by a number of ocular tissues. Unpublished microarray studies from our laboratory identified *Mfap2* (the gene encoding Magp1) as a moderately abundant transcript in the lens epithelium and Lattin *et. al*. have reported relatively high levels of *Mfap2* RNA in lens, ciliary body, and iris.[37]

A novel finding in our study was the observation that *Fbn2* mRNA was abundant in the embryonic mouse ciliary epithelium and that Fbn2 protein was readily detected in mouse zonular fibers. Proteomic analysis of zonular fibers from bovine and human eyes detected only the presence of Fbn1,[15] suggesting that the incorporation of Fbn2 into zonular fibers might be unique to the murine eye. In this regard, it is worth noting that although mutations in the human *FBN1* gene are associated with ectopia lentis, mutations in *FBN2* are not. *FBN2* mutations underlie Beal's syndrome (also known as congenital contractural arachnodactyly; CCA),[38] a condition characterized by contracture of the joints. Patients with Beal's syndrome are prone to many of the skeletal and vascular problems that MS patients face, but few ocular complications have been reported.

Interpretation of immunofluorescence images of the developing eye was confounded initially by the unexpected observation that cells of the hyaloid vasculature expressed fibrillin (primarily *Fbn2*) and that the TVL and PM were rich in microfibrils. The matrices in which the microfibrils were embedded regressed over the first few weeks of postnatal development.[30] Presumably, the microfibrils were removed by extracellular proteolysis, although if this is the case, it is unclear how nascent zonular fibers, which presumably have a similar chemical composition, were spared. The switch from *Fbn2* to *Fbn1* expression observed during ciliary epithelium development has been observed in other developing systems.[39,40] In the case of the ciliary zonule, it was expected that isoform switching might result in zonular fibers in which the relative proportion of Fbn1 and Fbn2 varied along the length of the fibers. Assuming that fibers grow from their proximal end (i.e., that newly synthesized fibrillin subunits are incorporated into fibers at or near the surface of the NPCE), we might have predicted that in adults the region of the zonule in contact

Investigative Ophthalmology & Visual Science

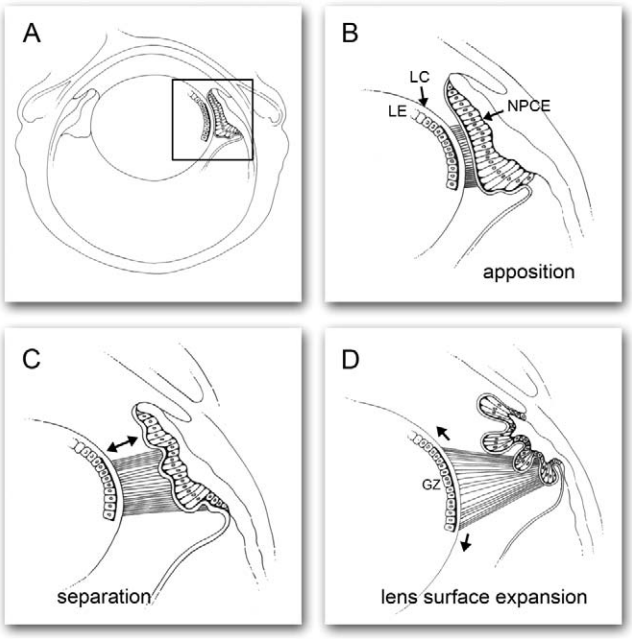

Figure 11. A simple model of ciliary zonule development. (**A**) By E16.5, an anatomically distinct ciliary epithelium is evident. (**B**) At this stage, the nonpigmented layer of the ciliary epithelium (NPCE) is closely apposed to the lens capsule (LC). Fibrillin-rich zonular fibers produced by the NPCE span the narrow cleft between the lens epithelium (LE) and the ciliary body and become intimately attached to the capsular surface. (**C**) Between P7 and P14, a sizable gap develops between the lens and the ciliary body. Continued addition of new components at the proximal (i.e., NPCE) ends of zonular fibers allows the fibers to lengthen and span the gap. (**D**) During postnatal development the lens surface area increases severalfold, whereas there is little or no increase in the surface of the NPCE region from which the zonular fibers originate. This causes the zonular fibers to fan out as they approach the lens. Zonular fibers are most sparse above the germinative zone, perhaps indicating that lens surface is added at a greater rate in this proliferatively active region than elsewhere.

with the lens would be relatively enriched in Fbn2 and that, conversely, the portion closest to the ciliary epithelium would be enriched in Fbn1 (the only isoform detected in the adult ciliary epithelium). However, we were not able to confirm this prediction by double-label immunofluorescence analysis. As predicted, *Fbn1* expression was diminished in regions close to the lens, but we did not detect a corresponding increase in the level of *Fbn2*. This may suggest that the hypothesis is wrong but could also be explained by the masking of Fbn2 epitopes in postnatal tissues, as described by others.[41] It will be important to clarify the distribution of Fbn2 along the zonular fibers because in vitro studies have suggested that fiber caliber is increased when fibrillin 2 is present.[42]

It has long been appreciated that a layer of fibrous material is present at the lens surface in the vicinity of the zonular attachment. This material was first observed by Berger in 1882, who referred to it as the *zonular lamellar*,[43] a term that has been used intermittently ever since. The present study provided insights into the substructure of this fibrous layer. Confocal imaging revealed that zonular fibers fanned out to contact the lens surface over an area 300 to 400 μm wide. Particularly noteworthy was the attachment zone of the posterior fibers, which we termed the fibrillar girdle. The girdle consisted of a ≍100-μm-wide band of densely packed, radially oriented microfibrils closely adherent to the capsular surface. Co-labeling with EdU, an S-phase marker, revealed that the girdle was located directly over the transition zone in the lens epithelium. In this region, epithelial cells withdraw from the cell cycle and commit to terminal differentiation.[33] Thus, the fibrillar girdle is uniquely situated to influence the growth of the lens. Work in other systems has shown that in addition to their well-documented structural roles, fibrillins regulate the bioavailability of TGFβ and Bone Morphogenetic Protein (BMP) family members.[44,45] In the lens, recent studies have demonstrated that a balance of BMP and FGF signaling is required for proper regulation of proliferation, cell cycle exit, and fiber cell differentiation.[46] Significantly, overexpression of noggin, an inhibitor of BMP signaling, led to loss of the polarized tissue organization and overgrowth of the lens epithelium.[47] Together, these data suggest that the arrangement of microfibrils on the capsular surface could subserve both structural and signaling functions by providing the rigging essential for lens centration while simultaneously targeting BMP signaling to specified regions of the lens epithelium.

The zonular apparatus is a complex arrangement of extracellular fibers that project from the surface of the NPCE to precise termination points on the lens capsule. It is not immediately evident how such an elaborate system could be erected across the gap that separates the lens from the ciliary body. Based on our data, we offer a general explanation for the genesis of the ciliary zonule (see Fig. 11). During embryonic and early postnatal development, the lens equator is in direct contact with the presumptive NPCE (Figs. 1–3, 7). At this stage, the nonpigmented epithelium is approximately 100 μm wide. We suggest that it is during this period, while the two tissues are in close contact, that strong connections are established between the lens capsule and nascent zonular fibers produced by the NPCE. The lens grows rapidly during early development but not as quickly as the overall dimensions of the eye. As a result, during the second postnatal week, a widening gap develops between the lens and the ciliary epithelium. During this period, fibrillin synthesis continues in the NPCE. The distal ends of the zonular fibers are already firmly attached to the lens capsule, and fibers grow in length by addition of fibrillin subunits at or near the surface of the NPCE. As a result, the zonular fibers are "fed out" across the developing gap. Although the lens surface area increases manyfold during early postnatal development, the field of NPCE cells synthesizing the zonular fibers does not markedly increase in size. This disparity in growth results in the characteristic "fanning out" of the zonular fibers as they approach the lens. The observation that zonular fibers are organized into two principal groups (anterior zonular fibers and posterior zonular fibers) may indicate that the lens surface area does not expand isotropically. The anterior and posterior fibers straddle the germinative zone of the lens, and it is possible that the surface increases more rapidly in this mitotically active region than elsewhere. An explicit test of this model will require pulse–chase experiments utilizing labeled capsule and zonule precursors.

In conclusion, the organization and composition of the mouse ciliary zonule are quite similar to those of the human. Future studies with mouse models should therefore provide meaningful insights into the genesis of the zonule, the role of fibrillin in modulating the growth of ocular structures, and the etiology of ocular defects in Marfan syndrome and related disorders.

Acknowledgments

The authors thank Linda Musil for her helpful comments on an early version of the manuscript.

Supported by National Institutes of Health Grants EY09852, EY018185 (SB), HL53325 and HL74138 (RPM), Core Grant for Vision Research P30 EY02687; and an unrestricted grant to the

Investigative Ophthalmology & Visual Science

Department of Ophthalmology and Visual Sciences from Research to Prevent Blindness.

Disclosure: **Y. Shi**, None; **Y. Tu**, None; **A. De Maria**, None; **R.P. Mecham**, None; **S. Bassnett**, None

References

1. Zinn J. *Descriptio Anatomica Oculi Humani Iconibus Illustrata*. Gottingen: Viduam B. Abrami Vandenhoeck; 1755.
2. McCulloch C. The zonule of Zinn: its origin, course, and insertion, and its relation to neighboring structures. *Trans Am Ophthalmol Soc*. 1954;52:525–585.
3. Streeten BW. The nature of the ocular zonule. *Trans Am Ophthalmol Soc*. 1982;80:823–854.
4. Streeten BW. Anatomy of the zonular apparatus. In: Tasman W, Jaeger E, eds. *Duane's Ophthalmology*. Vol. 1. Philadelphia, PA: Lippincott Williams and Wilkins; 2011.
5. Fullmer HM, Lillie RD. The oxytalan fiber: a previously undescribed connective tissue fiber. *J Histochem Cytochem*. 1958;6:425–430.
6. Hansson HA. Scanning electron microscopy of the zonular fibers in the rat eye. *Z Zellforsch Mikrosk Anat*. 1970;107:199–209.
7. Rohen JW. Scanning electron microscopic studies of the zonular apparatus in human and monkey eyes. *Invest Ophthalmol Vis Sci*. 1979;18:133–144.
8. Bornfeld N, Spitznas M, Breipohl W, Bijvank GJ. Scanning electron microscopy of the zonule of Zinn. I. Human eyes. *Albrecht Von Graefes Arch Klin Exp Ophthalmol*. 1974;192:117–129.
9. Bernal A, Parel JM, Manns F. Evidence for posterior zonular fiber attachment on the anterior hyaloid membrane. *Invest Ophthalmol Vis Sci*. 2006;47:4708–4713.
10. Ludwig K, Wegscheider E, Hoops JP, Kampik A. In vivo imaging of the human zonular apparatus with high-resolution ultrasound biomicroscopy. *Graefes Arch Clin Exp Ophthalmol*. 1999;237:361–371.
11. Lutjen-Drecoll E, Kaufman PL, Wasielewski R, Ting-Li L, Croft MA. Morphology and accommodative function of the vitreous zonule in human and monkey eyes. *Invest Ophthalmol Vis Sci*. 2010;51:1554–1564.
12. Nankivil D, Manns F, Arrieta-Quintero E, et al. Effect of anterior zonule transection on the change in lens diameter and power in cynomolgus monkeys during simulated accommodation. *Invest Ophthalmol Vis Sci*. 2009;50:4017–4021.
13. Sakai LY, Keene DR, Engvall E. Fibrillin, a new 350-kD glycoprotein, is a component of extracellular microfibrils. *J Cell Biol*. 1986;103:2499–2509.
14. Gibson MA, Cleary EG. The immunohistochemical localisation of microfibril-associated glycoprotein (MAGP) in elastic and non-elastic tissues. *Immunol Cell Biol*. 1987;65(pt 4):345–356.
15. Cain SA, Morgan A, Sherratt MJ, Ball SG, Shuttleworth CA, Kielty CM. Proteomic analysis of fibrillin-rich microfibrils. *Proteomics*. 2006;6:111–122.
16. Jensen SA, Robertson IB, Handford PA. Dissecting the fibrillin microfibril: structural insights into organization and function. *Structure*. 2012;20:215–225.
17. Jacob MP. Alterations of elastic fibers in genetically modified mice and human genetic diseases. *Front Biosci (Elite Ed)*. 2011;3:994–1004.
18. Collod-Beroud G, Le Bourdelles S, Ades L, et al. Update of the UMD-FBN1 mutation database and creation of an FBN1 polymorphism database. *Hum Mutat*. 2003;22:199–208.
19. Maumenee IH. The eye in the Marfan syndrome. *Birth Defects Orig Artic Ser*. 1982;18:515–524.
20. Loeys BL, Dietz HC, Braverman AC, et al. The revised Ghent nosology for the Marfan syndrome. *J Med Genet*. 2010;47:476–485.
21. Neptune ER, Frischmeyer PA, Arking DE, et al. Dysregulation of TGF-beta activation contributes to pathogenesis in Marfan syndrome. *Nat Genet*. 2003;33:407–411.
22. Shaner NC, Campbell RE, Steinbach PA, Giepmans BN, Palmer AE, Tsien RY. Improved monomeric red, orange and yellow fluorescent proteins derived from Discosoma sp. red fluorescent protein. *Nat Biotechnol*. 2004;22:1567–1572.
23. Muzumdar MD, Tasic B, Miyamichi K, Li L, Luo L. A global double-fluorescent Cre reporter mouse. *Genesis*. 2007;45:593–605.
24. Weinbaum JS, Broekelmann TJ, Pierce RA, et al. Deficiency in microfibril-associated glycoprotein-1 leads to complex phenotypes in multiple organ systems. *J Biol Chem*. 2008;283:25533–25543.
25. Arteaga-Solis E, Gayraud B, Lee SY, Shum L, Sakai L, Ramirez F. Regulation of limb patterning by extracellular microfibrils. *J Cell Biol*. 2001;154:275–281.
26. Bassnett S, Shi Y. A method for determining cell number in the undisturbed epithelium of the mouse lens. *Mol Vis*. 2010;16:2294–2300.
27. Charbonneau NL, Dzamba BJ, Ono RN, et al. Fibrillins can co-assemble in fibrils, but fibrillin fibril composition displays cell-specific differences. *J Biol Chem*. 2003;278:2740–2749.
28. Wang F, Flanagan J, Su N, et al. RNAscope: a novel in situ RNA analysis platform for formalin-fixed, paraffin-embedded tissues. *J Mol Diagn*. 2012;14:22–29.
29. Corson GM, Charbonneau NL, Keene DR, Sakai LY. Differential expression of fibrillin-3 adds to microfibril variety in human and avian, but not rodent, connective tissues. *Genomics*. 2004;83:461–472.
30. Ito M, Yoshioka M. Regression of the hyaloid vessels and pupillary membrane of the mouse. *Anat Embryol (Berl)*. 1999;200:403–411.
31. Hiraoka M, Inoue K, Ohtaka-Maruyama C, et al. Intracapsular organization of ciliary zonules in monkey eyes. *Anat Rec (Hoboken)*. 2010;293:1797–1804.
32. Harding CV, Hughes WL, Bond VP, Schork P. Autoradiographic localization of tritiated thymidine in wholemount preparations of lens epithelium. *Arch Ophthalmol*. 1960;63:58–65.
33. Mikulicich AG, Young RW. Cell proliferation and displacement in the lens epithelium of young rats injected with tritiated thymidine. *Invest Ophthalmol*. 1963;2:344–354.
34. Lovicu FJ, McAvoy JW. Growth factor regulation of lens development. *Dev Biol*. 2005;280:1–14.
35. Hanssen E, Franc S, Garrone R. Synthesis and structural organization of zonular fibers during development and aging. *Matrix Biol*. 2001;20:77–85.
36. Gloor BP. Radioisotopes for research into vitreous and zonule. *Adv Ophthalmol*. 1978;36:63–73.
37. Lattin JE, Schroder K, Su AI, et al. Expression analysis of G protein-coupled receptors in mouse macrophages. *Immunome Res*. 2008;4:5.
38. Putnam EA, Zhang H, Ramirez F, Milewicz DM. Fibrillin-2 (FBN2) mutations result in the Marfan-like disorder, congenital contractural arachnodactyly. *Nat Genet*. 1995;11:456–458.
39. Zhang H, Hu W, Ramirez F. Developmental expression of fibrillin genes suggests heterogeneity of extracellular microfibrils. *J Cell Biol*. 1995;129:1165–1176.
40. Mariencheck MC, Davis EC, Zhang H, et al. Fibrillin-1 and fibrillin-2 show temporal and tissue-specific regulation of expression in developing elastic tissues. *Connect Tissue Res*. 1995;31:87–97.

41. Charbonneau NL, Jordan CD, Keene DR, et al. Microfibril structure masks fibrillin-2 in postnatal tissues. *J Biol Chem*. 2010;285:20242–20251.
42. Yamanouchi K, Tsuruga E, Oka K, Sawa Y, Ishikawa H. Fibrillin-1 and fibrillin-2 are essential for formation of thick oxytalan fibers in human nonpigmented ciliary epithelial cells in vitro. *Connect Tissue Res*. 2012;53:14–20.
43. Berger E. Beiträge zur Anatomie der Zonula Zinnii. *Albrecht Von Graefes Arch Ophth*. 1882;28:28–62.
44. Nistala H, Lee-Arteaga S, Smaldone S, et al. Fibrillin-1 and –2 differentially modulate endogenous TGF-beta and BMP bioavailability during bone formation. *J Cell Biol*. 2010;190:1107–1121.
45. Ramirez F, Sakai LY. Biogenesis and function of fibrillin assemblies. *Cell Tissue Res*. 2010;339:71–82.
46. Jarrin M, Pandit T, Gunhaga L. A balance of FGF and BMP signals regulates cell cycle exit and Equarin expression in lens cells. *Mol Biol Cell*. 2012;23:3266–3274.
47. Boswell BA, Overbeek PA, Musil LS. Essential role of BMPs in FGF-induced secondary lens fiber differentiation. *Dev Biol*. 2008;324:202–212.

Investigative Ophthalmology & Visual Science